18

Skin Roughness Assessment

Lioudmila Tchvialeva[a], Haishan Zeng[a,b], Igor Markhvida[a], David I McLean[a], Harvey Lui[a,b] and Tim K Lee[a,b]
[a]*Laboratory for Advanced Medical Photonics and Photomedicine Institute, Department of Dermatology and Skin Science, University of British Columbia and Vancouver Coastal Health Research Institute, Vancouver, Canada*
[b]*Cancer Control and Cancer Imaging Departments, British Columbia Cancer Research Centre, Vancouver, Canada*

1. Introduction

The medical evaluation and diagnosis of skin disease primarily relies on visual inspection for specific lesional morphologic features such as color, shape, border, configuration, distribution, elevation, and texture. Although physicians and other health care professionals can apply classification rules to visual diagnosis (Rapini, 2003) the overall clinical approach is subjective and qualitative, with a critical dependence on training and experience. Over the past 20 years a number of non-invasive techniques for measuring the skin's physical properties have been developed and tested to extend the accuracy of visual assessment alone. Skin relief, also referred to as surface texture or topography, is an important biophysical feature that can sometimes be difficult to appreciate with the naked eye alone. Since the availability of quantification tools for objective skin relief evaluation, it has been learned that skin roughness is influenced by numerous factors, such as lesion malignancy (Connemann et al., 1995; Handels et al., 1999; del Carmen Lopez Pacheco et al., 2005; Mazzarello et al., 2006), aging (Humbert et al., 2003; Lagarde et al., 2005; Li et al., 2006a; Fujimura et al., 2007), diurnal rhythm and relative humidity (Egawa et al., 2002), oral supplement (Segger & Schonlau, 2004), cosmetics and personal care products (Korting et al., 1991; Levy et al., 2004; Kampf & Ennen, 2006; Kim et al., 2007; Kawada et al., 2008), laser remodeling (Friedman et al., 2002a), and radiation treatment (Bourgeois et al., 2003).

Two early surveys (Fischer et al., 1999; Leveque, 1999) reviewing assessment methods for topography were published a decade ago. In this chapter, we update current research techniques along with commercially-available devices, and focus on the state-of-the-art methods. The first part of the chapter analyzes indirect replica-based and direct *in-vivo* techniques. Healthy skin roughness values obtained by different methods are compared, and the limitations of each technique are discussed. In the second part, we introduce a novel approach for skin roughness measurement using laser speckle. This section consists of a survey on applying speckle for opaque surfaces, consideration of the theoretical relationship

between polychromatic speckle contrast and roughness, and a critical procedure for eliminating volume-scattering from semi-transparent tissues. Finally we compare roughness values for different body sites obtained by our technique to other *in-vivo* methods. Limitations of each technique and their practical applicability are discussed throughout the chapter.

2. Skin surface evaluation techniques

According to the International Organization for Standardization (ISO), methods for surface texture measurement are classified into three types: line profiling, areal topography, and area-integrating (International Organization for Standardization Committee, 2007). Line-profiling uses a small probe to detect the peaks and valleys and produces a quantitative height profile Z(x). Areal topography methods create 2 dimensional Z(x,y) topographic images. To compare surfaces, we have to analyse and calculate statistical parameters from the 2D maps. On the other hand, area-integrated methods capture an area-based signal and relate it directly to one or more statistical parameters without detailed point-by-point analysis of the surface.

ISO defines a set of parameters characterizing the roughness, which is the variation of the Z coordinate (height) from the mathematical point of view. We will discuss three of them: arithmetical mean deviation R_a, root mean square (rms) deviation R_q, and maximum height of profile R_z. Line profiling and areal topography methods commonly use R_a, which is the average of the absolute values $|Z - \langle Z \rangle|$ within the sampling region and $\langle Z \rangle$ is the average surface height. Theoretical formulations of the area-integrating methods mostly utilize $R_q = (\langle (Z - \langle Z \rangle)^2 \rangle)^{1/2}$,which is a statistical measure of the Z variation within the sampling region. The parameters R_a and R_q are highly correlated, for example $R_a \approx 1.25\ R_q$ when Z has a Gaussian distribution. Some applications employ the maximum height of the profile (R_z), which is defined as the distance between the highest peak and the lowest valley within a sampling region.

From the technical point of view, skin roughness can be measured directly (*in-vivo*) or indirectly from a replica. Replica-based methods were the first to be developed and implemented, and are still commonly used today despite the recent advancements in *in-vivo* techniques and devices. Therefore, we discuss both approaches in the following section.

2.1 Replica-based methods

Replica-based methods require two-steps. Skin surface has to be imprinted and a skin replica is produced. Roughness measurement is then performed on the replica. The most commonly used material for the replica is silicone rubber (Silfo®, Flexico Developments Ltd., UK). Silicon dental rubber (Silasoft®, Detax GmbH & Co., Gemany) (Korting, et al., 1991), polyvinylsiloxane derivative (Coltene®, Coltène/Whaledent Ltd., UK) (Mazzarello, et al., 2006), and silicon mass (Silaplus®, DMG, Gamany) (Hof & Hopermann, 2000) have also been used. The comparison between Flexico and DMG silicones revealed a good agreement (Hof & Hopermann, 2000).

The range of skin topography dictates the choice of technical approaches for the assessment. According to the classification given in (Hashimoto, 1974), the surface pattern of the human

skin can be divided into primary structure, which consists of primary macroscopic, wide, deep lines or furrows in the range of 20 μm to 100 μm, secondary structure formed by finer, shorter and shallower (5 μm - 40 μm) secondary lines or furrows running over several cells, tertiary structure lines (0.5 μm) that are the borders of the individual horny cells, and quaternary lines (0.05 μm) on individual horny cells surfaces. The range of the skin roughness value, as expected, is mainly determined by the primary and secondary structures which are in the order of tens of microns. These structures can be examined by mechanical profilometry with a stylus. The tertiary and quaternary structures do not visibly contribute to the roughness parameters, but causes light to be reflected diffusively. In order to evaluate these fine structures, optical techniques should be employed (Hocken et al., 2005).

2.1.1 Line Profile – contact method

Mechanical profilometry is a typical line-profiling approach. The stylus tip follows the surface height directly with a small contacting force. The vertical motion on the stylus is converted to an electrical signal, which is further transformed into the surface profile Z(x). The smallest vertical resolution is 0.05 μm (Hof & Hopermann, 2000). The best lateral resolution is 0.02 μm, which is limited by the size of the stylus tip. The finite tip size causes smoothing in valleys (Connemann et al., 1996) but peaks can be followed accurately. The stylus may damage or deform the soft silicone rubber. Nevertheless, due to its high accuracy and reliability, mechanical profilometry is still in use since an early study reported in the 1990s (Korting, et al., 1991).

2.1.2 Areal Topography - optical techniques

Microphotography is the easiest way to image skin texture and works well with the anisotropy of skin furrows (Egawa, et al., 2002) or the degree of skin pattern irregularity (Setaro & Sparavigna, 2001). In a study (Mazzarello, et al., 2006), surface roughness is presented as a non-ISO parameter by the standard deviation of the grey level of each pixel in a scanning electron microscopy image. In optical shadow casting (Gautier et al., 2008), a skin replica is illuminated by a parallel light beam with at a non-zero incident angle and the cast shadow length is directly related to the height of the furrows. Surface mapping can be done by simple trigonometric calculations (del Carmen Lopez Pacheco, et al., 2005). However, this method cannot detect relief elements located inside the shadowed areas. Its resolution depends on the incident angle and is lower than other optical methods. Some microphotography studies reported extreme values. For example the value R_a averaged over different body sites has been reported as high as 185.4 μm (del Carmen Lopez Pacheco, et al., 2005), which was by an order of magnitude greater than the commonly accepted values (Lagarde, et al., 2005). Another study on forearm skin (Gautier, et al., 2008) reported a very low R_z value, 8.7 μm, which was by an order of magnitude lower than the common range (Egawa, et al., 2002). Currently, microphotography is primarily used for wrinkle evaluation.

Optical profilometry is based on the autofocus principle. An illumination-detection system is focused on a flat reference plane. Any relief variation will result in image defocusing and decrease the signal captured by a detector. Automatic refocusing is then proceeded by shifting the focusing lens in the vertical direction. This shift is measured at each point (x,y) and then converted to surface height distribution Z(x,y). The presicion of laser profilometers

(Connemann, et al., 1995; Humbert, et al., 2003) is very high: vertical resolution of 0.1 μm (up to 1 nm) with a measurement range of 1 mm, and lateral resolution of 1 μm with a horizontal range up to 4 mm. However this performance requires about 2 hours of sampling time for a 2 mm × 4 mm sample (Humbert, et al., 2003). In addition, a study showed that the roughness value is sensitive to the spatial frequency cut-off and sampling interval during the signal processing (Connemann, et al., 1996). The new confocal microscopy approach used by (Egawa, et al., 2002) reduces the sampling time to a few minutes. However, the new approach inherits the same disadvantages in signal processing with regards to the wavelength cut-off and sampling interval.

The light transmission method records the change of transparency of thin (0.5 mm) silicone replicas (Fischer, et al., 1999). The thickness of relief is calculated according to the Lambert-Beer Law for the known absorption of the transmitted parallel light. The advantages of this method are the relatively short processing time (about 1 min), and good performance: vertical resolution is 0.2 μm with a range of 0.5 mm, and lateral resolution is 10 μm with a horizontal range up to 7.5 mm. A commercial device is available. However, making thin replicas requires extra attention over a multi-step procedure. Analyzing the gray level of the transmission image provides relative, but not the standard ISO roughness parameters (Lee et al., 2008). Furthermore, volume-scattered light introduces noise that must be suppressed by a special image processing step (Articus et al., 2001).

The structured light and triangulation technique combines triangulation with light intensity modulation using sinusoidal functions (Jaspers et al., 1999). Triangulation methodology uses three reference points: the source, surface, and image point. Variation along the height of the surface points alters their positions on the detector plane. The shift is measured for the entire sample and is transformed to a Z(x,y) map. The addition of modulated illumination light intensity (fringe projection) allows the use of a set of micro photos with different fringe widths and avoids point-to-point scanning. The acquisition time drops to a few seconds. This technique has been applied to skin replica micro-relief investigation in many studies (Lagarde, et al., 2005; Li, et al., 2006a; Kawada, et al., 2008).

2.1.3 Area-integrating methods

Industrial application of area-integrating methods has been reported (Hocken, et al., 2005), but the technique has not been applied for skin replicas prior to our laser speckle method, which will be described in detail in the second half of this chapter. Although the laser speckle method is designed for *in-vivo* measurement, it can be used for skin replicas.

2.2 *In-vivo* methods

Because replica-based methods are inconvenient in clinical settings and susceptible to distortions during skin relief reproduction, direct methods are preferable. However, data acquisition speed is one of the critical criteria for *in-vivo* methods. Many replica-based methods such as mechanical profilometry, optical profilometry, and light transmission cannot be applied *in-vivo* to skin because of their long scanning times. A review article (Callaghan & Wilhelm, 2008) divided the existing *in-vivo* methods into three groups: videoscopy (photography), capacitance mapping, and fringe projection methods. Videoscopy provides 2D grayscale micro (Kim, et al., 2007) or macro (Bielfeldt et al., 2008)

photographs for skin texture analysis. Capacitive pixel-sensing technology (SkinChip®, (Leveque & Querleux, 2003), an area-integrating surface texture method, images a small area of about 50 μm and exposes skin pores, primary and secondary lines, and wrinkles, etc. Unfortunately, both approaches are unable to quantify roughness according to the ISO standards and therefore they are rarely applied. To the best of our knowledge, the only technique widely used today for *in-vivo* skin analysis is fringe projection areal topography.

2.2.1 Fringe projection

The first in-vivo line profiling optical device based on the triangulation principle was introduced in (Leveque & Querleux, 2003). The lateral resolution and vertical range were designed to be 14 μm and 1.8 mm, respectively. The scanning time was up to 5 mm/sec. However, the device was not commercialized because it was too slow for analyzing area roughness and not portable. After combining this triangulation device with illumination by sinusoidal light (fringe pattern projection), and recording several phase-shifted surface images, the acquisition time was reduced to less than 1 second; commercial area topography systems was now feasible. Currently, two such devices are available on the market: PRIMOS® (GFMesstechnik GmbH, Berlin, Germany) and DermaTOP® (Breuckmann, Teltow, Germany). The main difference between them is in how the fringe patterns are produced: the PRIMOS® uses micro-mirrors with different PRIMOS® models available according to sampling sizes (Jaspers, et al., 1999), while DermaTOP® uses a template for the shadow projection and offers the option of measuring different sized areas using the same device (Lagarde et al., 2001). Similar performances are reported by both systems. DermaTOP® shows the highest performance for measuring an area of 20 × 15 mm^2. It achieves 2 μm for vertical resolution and 15 μm for lateral resolution with an acquisition time less than 1 second (Rohr & Schrader, 1998). The PRIMOS® High Resolution model examines a 24 × 14 mm^2 area in 70 ms with a vertical resolution of 2.4 μm, and lateral resolution of 24 μm (Jacobi et al., 2004). The drawbacks for fringe projection are interference of back scattering from skin tissue volume effects, micro movement of the body which deforms the fringe image and concern over the accuracy due to moderate resolution.

2.2.2 Comparing replica and *in-vivo* skin roughness results

Evaluating devices that measure skin roughness requires the consideration of a reference gold standard for the "true" skin roughness. The skin is difficult to study *in-vivo* and therefore the first roughness measurements were simply done on skin replicas with the assumption that they were faithful reproductions. Unfortunately replicas represent low pass filters due to the material viscosity that causes some loss of finer relief structure, ultimately leading to lower replica roughness values than direct *in-vivo* roughness measurements (Hof & Hopermann, 2000). This effect was reported in (Rohr & Schrader, 1998; Hof & Hopermann, 2000; Friedman et al., 2002b). The uncertainty introduced by replicas in roughness measurements was estimated as 10% (Lagarde, et al., 2001). In Figure 1 we plot the literature data for replica roughness and *in-vivo* roughness for three body sites. The arithmetical mean roughness was measured by PRIMOS® (Hof & Hopermann, 2000; Friedman, et al., 2002b; Rosén et al., 2005) and DermaTOP® (Rohr & Schrader, 1998), directly and from replicas of the same area.

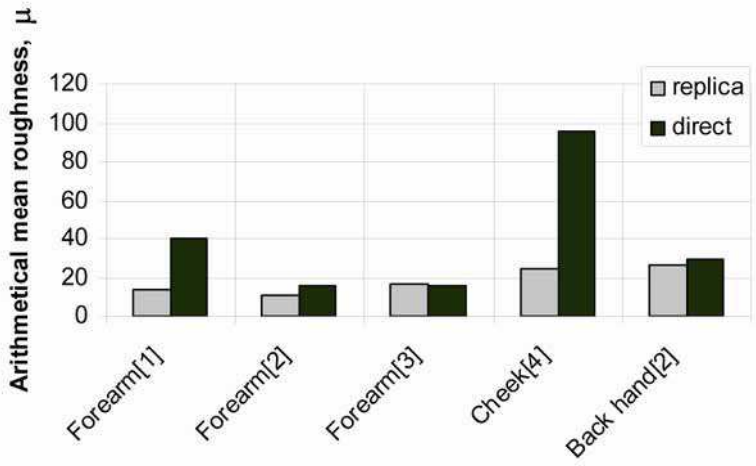

Fig. 1. Direct *in-vivo* roughness (■ direct) and replica roughness (□ replica) for three different body sites. [1]: (Rohr & Schrader, 1998); [2]: (Hof & Hopermann, 2000); [3]: (Rosén et al., 2005); [4]: (Friedman et al., 2002b).

The first three column pairs depict roughness data taken from volar forearm skin. As reported by (De Paepe et al., 2000; Lagarde, et al., 2001; Egawa, et al., 2002; Lagarde, et al., 2005) the skin roughness of the volar forearm has more consistent characteristics and does not vary significantly with age or gender: by only from 13% (Jacobi, et al., 2004) up to 20% (De Paepe, et al., 2000). Comparing the three different studies, we observed that the spread of the replica roughness is close to 20%, whereas the variability of the *in-vivo* roughness substantially exceeds the upper bound of 20%. Figure 1 also shows a large difference between *in-vivo* roughness and replica roughness in a study involving forearm skin (Rohr & Schrader, 1998) which was conducted with DermaTOP®, and another study of the cheek (Friedman, et al., 2002b) measured by PRIMOS®. These large discrepancies may have many different causes including those of replica and *in-vivo* methods indicated in the previous sections, but they also suggest that further investigations in the area of *in-vivo* skin micro-relief measurement are required.

3. In-vivo skin roughness measured by speckle

In this section, we introduce a novel approach to skin roughness assessment by laser speckle. When surface profiling is not necessary, speckle techniques are popular in industry for surface assessment because the techniques deploy a low cost and simple imaging device which allows a fast sampling time. Speckle methods are classified as an area-integrating optical technique for direct measurements. We first examine various speckle techniques used in industrial applications, and classify them according to their designated roughness range. Then we discuss the adaptation of the technique to *in-vivo* skin measurement.

3.1 Speckle application for opaque surfaces

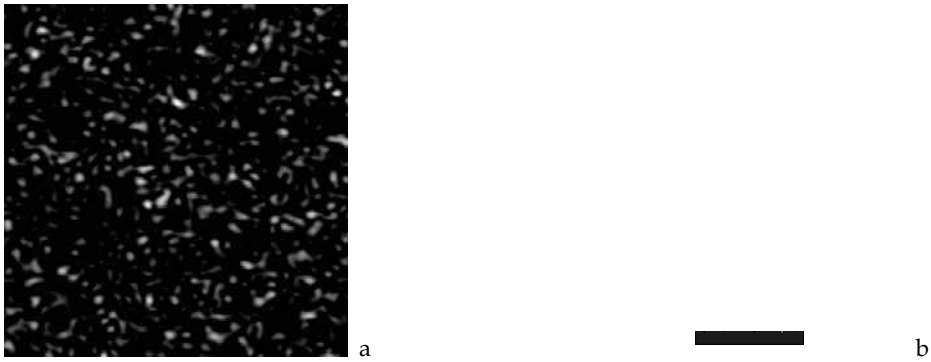

Fig. 2. Speckle pattern (a) and optical setup for speckle measurements (b)

Speckle is a random distribution of intensity of coherent light that arises by scattering from a rough surface.
Fig. **2** shows a typical speckle pattern (a) and an optical setup (b) for obtaining the speckle signal, which in turn contains information about roughness.

Speckle theories for roughness measurement were established a couple of decades ago and were reviewed in (Briers, 1993). However these theories had not been developed into practical instruments in the early years due to technical issues. Recent developments in light sources and registration devices have now revived interest in speckle techniques.

In general, these techniques can be categorized into two approaches: a) finding differences or similarities for two or more speckle patterns and b) analyzing the properties of a speckle pattern.

3.1.1 Correlation methods

Correlation methods analyze the decorrelation degree of two or more speckle images produced under different experimental conditions by altering the wavelength (Peters & Schoene, 1998), the angle of illumination (Death et al., 2000), or the microstructure of surfaces using different surface finishes (Fricke-Begemann & Hinsch, 2004). Although these methods hold a solid theoretical foundation, they are not suitable for *in-vivo* skin examination. One of the reasons is that internal multiply scattering contributes significantly to the total speckle decorrelation.

3.1.2 Speckle image texture analysis

The speckle photography approach analyzes features on a single speckle pattern. The analysis may include assessments of speckle elongation (Lehmann, 2002), co-occurrence matrices (Lu et al., 2006), fractal features of the speckle pattern (Li et al., 2006b), or the mean size of "speckled" speckle (Lehmann, 1999). A speckle image can be captured easily by a camera when a light source illuminates a surface and a speckle pattern is formed. The main

drawback of the approach is that the relationships between most of the texture patterns and surface roughness, except (Lehmann, 2002), were established empirically. As a result, the success of this approach entirely depends on a rigid image formation set up and a careful and detailed calibration between the texture features and surface roughness. In addition, these "ad-hoc" assessments do not conform to the ISO standards.

3.1.3 Speckle contrast techniques

Speckle contrast (see detailed definition in Section 3.2.1) is a numerical value that can be easily measured and is well-described theoretically. It depends on the properties of the light source, surface roughness and the detector. Surface parameters can be recovered from the measured contrast. (Goodman, 2006).

From a physics point of view, there are two situations that can change (decrease) the contrast of a speckle pattern. One is to decrease the path difference between the elementary scattered waves in comparison with their wavelengths. This is the so-called weak-scattering surface condition which is used in many earlier practical applications (Fujii & Asakura, 1977) based on monochromatic light. A recent modification of this method gives a useful analytical solution for speckle contrast in terms of surface roughness, aperture radius and lateral-correlation length (Cheng et al., 2002). The weak-scattering condition limits the measurable roughness to no larger than 0.3 times the illuminating wavelength. The upper limit of surface roughness can be raised by a factor of 4 for a high angle of incidence light (Leonard, 1998). However the light wavelength introduces the natural upper limit of the measurable roughness range for weak-scattering methods. There have been few attempts to increase the detection range while also achieving quantitative results at the same time. In one case, a complex two-scale surface structure was studied (Hun et al., 2006), and in another case, the results conflicted with the speckle theory (Lukaszewski et al., 1993).

The second scenario for contrast alternation is to increase the path difference of the elementary scattered waves, up to the order of the coherence length of the light source. Implementation of this technique is based on a polychromatic source of light with finite coherence. Known practical realization of this technique covers only a narrow range of few microns (Sprague, 1972).

The measurable roughness ranges reported in the literature are plotted in Figure 3. The chart shows that the majority of the existing speckle methods are sensitive to the submicron diapason. Only the angle correlation technique accessed roughness up to 20 microns. To evaluate skin, whose roughness may be up to 100 microns, a new approach is needed.

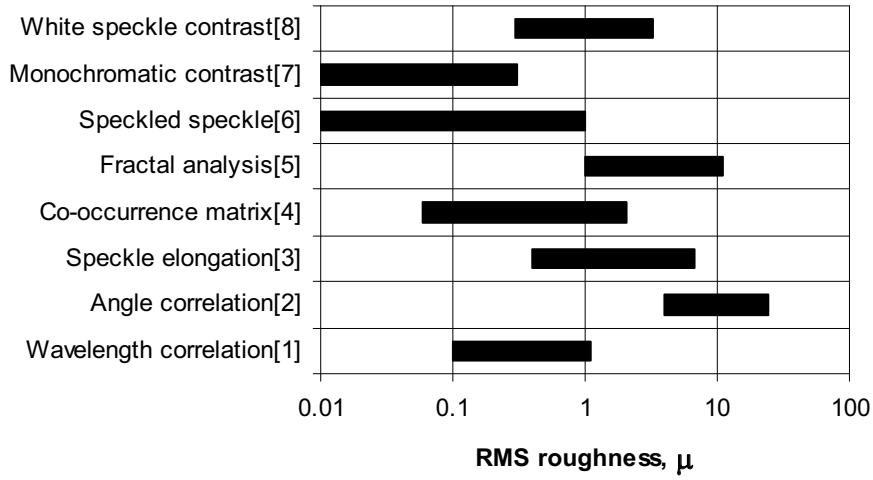

Fig. 3. Chart for roughness range achieved by existing speckle techniques. The roughness range is in a log scale. [1]: (Peters & Schoene,1998); [2]: (Death et al., 2000); [3]: (Lehmann, 2002); [4]: (Lu et al., 2006b); [5]: (Li et al., 2006b); [6]: (Lehmann, 1999); [7]: (Fujii & Asakura, 1977); [8]: (Sprague, 1972).

3.2 Skin roughness measurement by speckle contrast

The possibility of measuring roughness within the range of the coherence length of a light source was experimentally demonstrated over three decades ago (Sprague, 1972). Later the theoretical formulation of this problem, i.e., relating contrast in terms of rms surface roughness R_q with a Gaussian spectral shape light source, was described by Parry (Parry, 1984). Therefore, the problem of measuring skin roughness, ranging from 10 μm up to 100 μm, becomes one of using an appropriate light source. A typical diode laser provides a coherence length of a few tens of microns and as such is suitable for skin testing. Unfortunately, a diode lasers' resonator is typically a Fabry-Perot interferometer with a multi-peak emission spectrum (Ning et al., 1992), which violates the Gaussian spectral shape assumption of Parry's theory. Therefore, we have to find a relation between R_q and the polychromatic speckle contrast for any light source with an arbitrary spectrum.

3.2.1 Extension of the speckle detection range

Contrast C of any speckle pattern is defined as (Goodman, 2006)

$$C = \frac{\sigma_I}{< I >} \tag{1}$$

where <…> denotes an ensemble averaging, and σ_I is the standard deviation of light intensity I, with σ_I^2 being the variance:

$$\sigma_I^2 = <I^2> - <I>^2. \tag{2}$$

Let us illuminate a surface with a polychromatic light source that has a finite spectrum and a finite temporal coherence length. The intensity of polychromatic speckles is the sum of the monochromatic speckle pattern intensities:

$$I(\boldsymbol{x}) = \int_0^\infty F(k)\, I(\boldsymbol{x}, k)\, \mathrm{d}k, \tag{3}$$

where k is wave number, $F(k)$ is the spectral line profile of the illuminating light, and $\boldsymbol{x}$ is a vector in the observation plane. Eq. (3) implies that the registration time is much greater than the time of coherence. In other words, speckle patterns created by individual wavelengths are incoherent and we summarize them on the intensity basis. The behavior of $I(\boldsymbol{x})$ depends on many factors. In some areas of the observation plane, intensity $I(\boldsymbol{x}, k)$ for all k will have the same distribution and the contrast of the resultant speckle pattern will be the same as the contrast of the single monochromatic pattern. In other areas the patterns will be shifted and their sum produces a smoothed speckle pattern with a reduced contrast. The second moment of the intensity $I(\boldsymbol{x})$ can be calculated using Eq. (3):

$$\langle I^2(\boldsymbol{x})\rangle = \int_0^\infty \int_0^\infty F(k_1)F(k_2)\, \langle I(\boldsymbol{x}, k_1)\, I(\boldsymbol{x}, k_2)\rangle\, \mathrm{d}k_1\, \mathrm{d}k_2. \tag{4}$$

Calculating the variance according to Eqs. (2) - (4) we obtain:

$$\sigma_I^2 = \langle I^2\rangle - \langle I\rangle^2 = \int_0^\infty \int_0^\infty F(k_1)F(k_2)\, [\langle I(\boldsymbol{x}, k_1)\, I(\boldsymbol{x}, k_2)\rangle - \langle I(\boldsymbol{x}, k_1)\rangle\langle I(\boldsymbol{x}, k_2)\rangle]\, dk_1 dk_2 \tag{5}$$

It has been shown in (Markhvida et al., 2007) that Eqs. (3)-(5) can be transformed to

$$C^2(R_q) = \frac{2\int_0^\infty (\int_0^\infty F(k)F(k+\Delta k)dk)\exp(-(2R_q\Delta k)^2)d\Delta k}{(\int_0^\infty F(k)dk)^2}, \tag{6}$$

Knowing the emission light source spectrum $F(k)$ and performing a simple numerical calculation of Eq. (6), the calibration curve for the contrast C vs. the rms roughness R_q can be obtained. To derive a calibration curve we performed a numerical integration of Eq. (6) with the experimental diode laser spectra converted to $F(k)$. The calculated dependencies of contrast on roughness for a blue, 405 nm, 20 mW laser (BWB-405-20E, B&WTek, Inc.) and a red, 663 nm fiber-coupled, 5 mW laser (57PNL054/P4/SP, Melles Griot Inc.) are shown in Figure 4**.** Analyzing the slopes of the calibration curves validates the effectiveness of both lasers up to 100 μm (unpublished observations). For a typical contrast error of 0.01, the best accuracy was estimated as 1 μm and 2 μm for the blue and red lasers, respectively. It should be noted that the calibration curve is generated using surface-reflected light and is validated

for opaque surfaces. However, in the case of *in-vivo* skin testing, the majority of incident light will penetrate the skin and thus a large portion of the remitted signal is from volume backscattering. This volume effect must be removed to avoid a large systematic error.

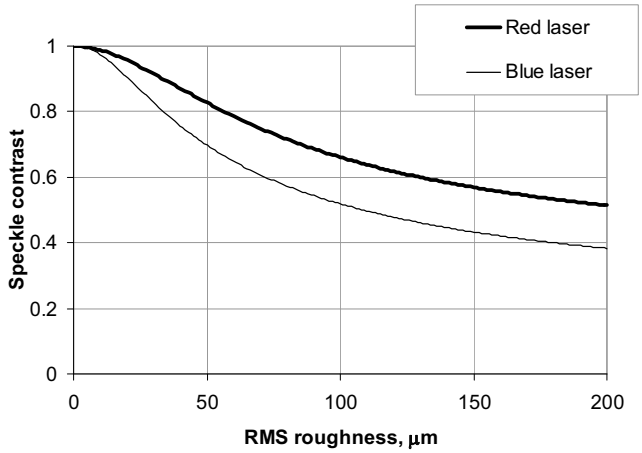

Fig. 4. The calculated contrast vs. R_q for a red and a blue diode lasers.

3.2.2 Separation of surface reflection from back-scattered light

The discrimination of light emerging from the superficial tissue from the light scattered in volume tissues is based on an assumption that the number of scatterings is correlated with the depth of penetration. The surface-reflected and subsurface scattered light is single scattered, whereas light emerging from the deeper volume is multiply-scattered. Three simple techniques for separating the single- and multiply-scattered light (spatial, polarization and spectral filtering) were recently established. Figure 5 illustrates how the filtering procedures work.

Spatial filtering relies on the property that single scattered light emerges at positions close to the illuminating spot (Phillips et al., 2005). Therefore the superficial signal can be enhanced by limiting the emerging light. Applying an opaque diaphragm centered at the incident beam allows the single scattered light from region 1 to be collected (Figure 5).

Polarization filtering is based on the polarization-maintaining property of single scattered light. When polarized light illuminates a scattering medium, the single scattered light emerging from the superficial region 1 maintains its original polarization orientation, while multiply scattered light emerging from a deeper region 2 possesses a random polarization state (Stockford et al., 2002).

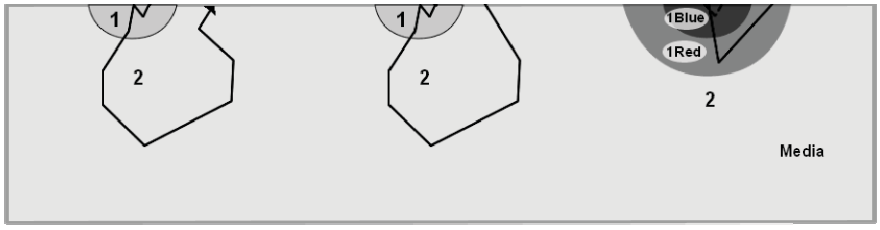

Fig. 5. Filtering principles of light propagating inside a biological tissue. Superficial and deep regions are marked as 1 and 2, respectively.

Registration of the co- and cross-linear polarizer output channels allows the determination of the degree of polarization (DOP), which is defined as:

$$DOP = \frac{< I_{\text{II}} > - < I_{\perp} >}{< I_{\text{II}} > + < I_{\perp} >} \tag{7}$$

where $<I_{\parallel}>$ and $<I_{\perp}>$ are the mean intensity of the co- and cross-polarized speckle patterns. Subtracting the cross-polarized pattern from the co-polarized pattern suppresses the volume scattering.

Spectral filtering (Demos et al., 2000) is based on the spectral dependence of skin attenuation coefficients (Salomatina et al., 2006). Shorter wavelengths are attenuated more heavily in a scattering medium and yield a higher output of scattered light than longer wavelengths. Therefore region 1 for the blue light is expected to be shallower than the red light, and, we should thus use the blue laser for skin roughness measurements (Tchvialeva et al., 2008).

In another study (Tchvialeva et al., 2009), we adopted the above filtering techniques for speckle roughness estimation of the skin. However, our experiment showed that the filtered signals still contained sufficient volume-scattered signals and overestimated the skin roughness. Therefore, we formulate a mathematical correction to further adjust the speckle contrasts to their surface reflection values.

3.2.3 Speckle contrast correction

The idea of speckle contrast correction for eliminating the remaining volume scattering was inspired by the experimental evidence arising from the co-polarized contrast vs. DOP as

shown in Figure 6 (Tchvialeva, et al., 2009). There is a strong correlation between the co-polarized contrast and DOP ($r = 0.777$, $p < 0.0001$).

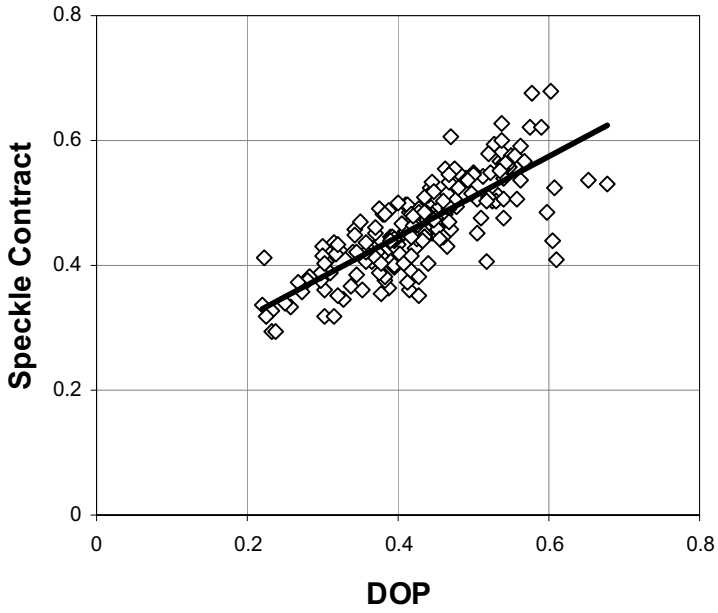

Fig. 6. The linear fit of the experimental points for co-polarized contrast vs. DOP.

We assume (at least as a first approximation) that this linear relation is valid for the entire range of DOP from 0 to 1. We also know that weakly scattered light has almost the same state of polarization as incident light (Sankaran et al., 1999; Tchvialeva, et al., 2008). If the incident light is linearly polarized (DOP = 1), light scattered by the surface should also have $DOP_{surf} = 1$. Based on this assumption, we can compute speckle contrast for surface scattered light by linearly extrapolating the data for DOP = 1. The corrected contrast is then applied to the calibration curve for the blue laser (Figure 4) and is mapped to the corrected roughness value.

3.2.4 Comparing *in-vivo* data for different body sites

To compare skin roughness obtained by our prototype with other *in-vivo* data, we conducted an experiment with 34 healthy volunteers. Figure 7 shows preliminary data for speckle roughness and standard deviation for various body sites. We also looked up the published *in-vivo* roughness values for the same body site and plot these values against our roughness measurements. Measured speckle roughness are consistent with published values. Currently, we are in the process of designing a study to compare the speckle roughness with replica roughness.

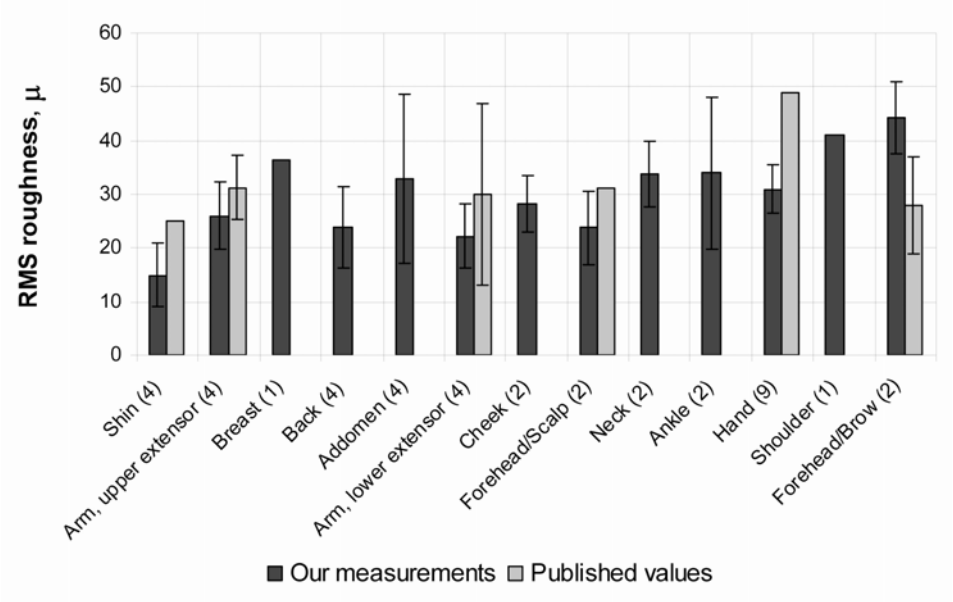

Fig. 7. In-vivo skin rms roughness obtained by our speckle device and by published values of fringe projection systems. The number of samples measured by the speckle prototype is denoted within the parentheses after the body sites.

4. Conclusion

Skin roughness is important for many medical applications. Replica-based techniques have been the *de facto* method until the recent development of fringe projection, an area-topography technique, because short data acquisition time is most crucial for *in-vivo* skin application. Similarly, laser speckle contrast, an area-integrating approach, also shows potential due to its acquisition speed, simplicity, low cost, and high accuracy. The original theory developed by Parry was for opaque surfaces and for light source with a Gaussian spectral profile. We extended the theory to polychromatic light sources and applied the method to a semi-transparent object, skin. Using a blue diode laser, with three filtering mechanisms and a mathematical correction, we were able to build a prototype which can measure rms roughness R_q up to 100 μm. We have conducted a preliminary pilot study with a group of volunteers. The results were in good agreement with the most popular fringe project methods. Currently, we are designing new experiments to further test the device.

5. References

Articus, K.; Brown, C. A. & Wilhelm, K. P. (2001). *Scale-sensitive fractal analysis using the patchwork method for the assessment of skin roughness*, *Skin Res Technol,* Vol. 7, No. 3, pp. 164-167

Bielfeldt, S.; Buttgereit, P.; Brandt, M.; Springmann, G. & Wilhelm, K. P. (2008). *Non-invasive evaluation techniques to quantify the efficacy of cosmetic anti-cellulite products*, *Skin Res Technol,* Vol. 14, No. 3, pp. 336-346

Bourgeois, J. F.; Gourgou, S.; Kramar, A.; Lagarde, J. M.; Gall, Y. & Guillot, B. (2003). *Radiation-induced skin fibrosis after treatment of breast cancer: profilometric analysis*, *Skin Res Technol,* Vol. 9, No. 1, pp. 39-42

Briers, J. (1993). Surface roughness evaluation. In: *Speckle Metrology, Sirohi, R. S.* (Eds), by CRC Press

Callaghan, T. M. & Wilhelm, K. P. (2008). *A review of ageing and an examination of clinical methods in the assessment of ageing skin. Part 2: Clinical perspectives and clinical methods in the evaluation of ageing skin*, *Int J Cosmet Sci,* Vol. 30, No. 5, pp. 323-332

Cheng, C.; Liu, C.; Zhang, N.; Jia, T.; Li, R. & Xu, Z. (2002). *Absolute measurement of roughness and lateral-correlation length of random surfaces by use of the simplified model of image-speckle contrast*, *Applied Optics,* Vol. 41, No. 20, pp. 4148-4156

Connemann, B.; Busche, H.; Kreusch, J.; Teichert, H.-M. & Wolff, H. (1995). *Quantitative surface topography as a tool in the differential diagnosis between melanoma and naevus*, *Skin Res Technol,* Vol. 1, pp. 180-186

Connemann, B.; Busche, H.; Kreusch, J. & Wolff, H. H. (1996). *Sources of unwanted variabilitv in measurement and description of skin surface topography*, *Skin Res Technol,* Vol. 2, pp. 40-48

De Paepe, K.; Lagarde, J. M.; Gall, Y.; Roseeuw, D. & Rogiers, V. (2000). *Microrelief of the skin using a light transmission method*, *Arch Dermatol Res,* Vol. 292, No. 10, pp. 500-510

Death, D. L.; Eberhardt, J. E. & Rogers, C. A. (2000). *Transparency effects on powder speckle decorrelation*, *Optics Express,* Vol. 6, No. 11, pp. 202-212

del Carmen Lopez Pacheco, M.; da Cunha Martins-Costa, M. F.; Zapata, A. J.; Cherit, J. D. & Gallegos, E. R. (2005). *Implementation and analysis of relief patterns of the surface of benign and malignant lesions of the skin by microtopography*, *Phys Med Biol,* Vol. 50, No. 23, pp. 5535-5543

Demos, S. G.; Radousky, H. B. & Alfano, R. R. (2000). *Deep subsurface imaging in tissues using spectral and polarization filtering*, *Optics Express,* Vol. 7, No. 1, pp. 23-28

Egawa, M.; Oguri, M.; Kuwahara, T. & Takahashi, M. (2002). *Effect of exposure of human skin to a dry environment*, *Skin Res Technol,* Vol. 8, No. 4, pp. 212-218

Fischer, T. W.; Wigger-Alberti, W. & Elsner, P. (1999). *Direct and non-direct measurement techniques for analysis of skin surface topography*, *Skin Pharmacol Appl Skin Physiol,* Vol. 12, No. 1-2, pp. 1-11

Fricke-Begemann, T. & Hinsch, K. (2004). *Measurement of random processes at rough surfaces with digital speckle correlation*, *J Opt Soc Am A Opt Image Sci Vis,* Vol. 21, No. 2, pp. 252-262

Friedman, P. M.; Skover, G. R.; Payonk, G. & Geronemus, R. G. (2002a). *Quantitative evaluation of nonablative laser technology*, *Semin Cutan Med Surg,* Vol. 21, No. 4, pp. 266-273

Friedman, P. M.; Skover, G. R.; Payonk, G.; Kauvar, A. N. & Geronemus, R. G. (2002b). *3D in-vivo optical skin imaging for topographical quantitative assessment of non-ablative laser technology*, *Dermatol Surg,* Vol. 28, No. 3, pp. 199-204

Fujii, H. & Asakura, T. (1977). *Roughness measurements of metal surfaces using laser speckle*, *JOSA,* Vol. 67, No. 9, pp. 1171-1176

Fujimura, T.; Haketa, K.; Hotta, M. & Kitahara, T. (2007). *Global and systematic demonstration for the practical usage of a direct in vivo measurement system to evaluate wrinkles*, *Int J Cosmet Sci,* Vol. 29, No. 6, pp. 423-436

Gautier, S.; Xhauflaire-Uhoda, E.; Gonry, P. & Pierard, G. E. (2008). *Chitin-glucan, a natural cell scaffold for skin moisturization and rejuvenation*, *Int J Cosmet Sci,* Vol. 30, No. 6, pp. 459-469

Goodman, J. W. (2006). *Speckle Phenomena in Optics: Theory and Application*, Roberts and Company Publishers

Handels, H.; RoS, T.; Kreusch, J.; Wolff, H. H. & Poppl, S. J. (1999). *Computer-supported diagnosis of melanoma in profilometry*, *Meth Inform Med,* Vol. 38, pp. 43-49

Hashimoto, K. (1974). *New methods for surface ultrastructure: Comparative studies of scanning electron microscopy, transmission electron microscopy and replica method*, *Int J Dermatol,* Vol. 13, No. 6, pp. 357-381

Hocken, R. J.; Chakraborty, N. & Brown, C. (2005). *Optical metrology of surface*, *CIRP Annals - Manufacturing Technology,* Vol. 54, No. 2, pp. 169-183

Hof, C. & Hopermann, H. (2000). *Comparison of replica- and in vivo-measurement of the microtopography of human skin*, *SOFW Journal,* Vol. 126, pp. 40-46

Humbert, P. G.; Haftek, M.; Creidi, P.; Lapiere, C.; Nusgens, B.; Richard, A.; Schmitt, D.; Rougier, A. & Zahouani, H. (2003). *Topical ascorbic acid on photoaged skin. Clinical, topographical and ultrastructural evaluation: double-blind study vs. placebo*, *Exp Dermatol,* Vol. 12, No. 3, pp. 237-244

Hun, C.; Bruynooghea, M.; Caussignacb, J.-M. & Meyrueisa, P. (2006). Study of the exploitation of speckle techniques for pavement surface, *Proc of SPIE 6341*, pp. 63412A,

International Organization for Standardization Committee (2007). *GPS-Surface texture:areal-Part 6: classification of methods for measuring surface structure, Draft 25178-6*

Jacobi, U.; Chen, M.; Frankowski, G.; Sinkgraven, R.; Hund, M.; Rzany, B.; Sterry, W. & Lademann, J. (2004). *In vivo determination of skin surface topography using an optical 3D device*, *Skin Res Technol,* Vol. 10, No. 4, pp. 207-214

Jaspers, S.; Hopermann, H.; Sauermann, G.; Hoppe, U.; Lunderstadt, R. & Ennen, J. (1999). *Rapid in vivo measurement of the topography of human skin by active image triangulation using a digital micromirror device mirror device*, *Skin Res Technol,* Vol. 5, pp. 195-207

Kampf, G. & Ennen, J. (2006). *Regular use of a hand cream can attenuate skin dryness and roughness caused by frequent hand washing*, *BMC Dermatol,* Vol. 6, pp. 1

Kawada, A.; Konishi, N.; Oiso, N.; Kawara, S. & Date, A. (2008). *Evaluation of anti-wrinkle effects of a novel cosmetic containing niacinamide*, *J Dermatol,* Vol. 35, No. 10, pp. 637-642

Kim, E.; Nam, G. W.; Kim, S.; Lee, H.; Moon, S. & Chang, I. (2007). *Influence of polyol and oil concentration in cosmetic products on skin moisturization and skin surface roughness*, *Skin Res Technol,* Vol. 13, No. 4, pp. 417-424

Korting, H.; Megele, M.; Mehringer, L.; Vieluf, D.; Zienicke, H.; Hamm, G. & Braun-Falco, O. (1991). *Influence of skin cleansing preparation acidity on skin surface properties*, *International Journal of Cosmetic Science,* Vol. 13, pp. 91-102

Lagarde, J. M.; Rouvrais, C. & Black, D. (2005). *Topography and anisotropy of the skin surface with ageing*, *Skin Res Technol,* Vol. 11, No. 2, pp. 110-119

Lagarde, J. M.; Rouvrais, C.; Black, D.; Diridollou, S. & Gall, Y. (2001). *Skin topography measurement by interference fringe projection: a technical validation*, *Skin Res Technol,* Vol. 7, No. 2, pp. 112-121

Lee, H. K.; Seo, Y. K.; Baek, J. H. & Koh, J. S. (2008). *Comparison between ultrasonography (Dermascan C version 3) and transparency profilometry (Skin Visiometer SV600)*, *Skin Res Technol,* Vol. 14, pp. 8-12

Lehmann, P. (1999). *Surface-roughness measurement based on the intensity correlation function of scattered light under speckle-pattern illumination*, *Applied Optics,* Vol. 38, No. 7, pp. 1144-1152

Lehmann, P. (2002). *Aspect ratio of elongated polychromatic far-field speckles of continuous and discrete spectral distribution with respect to surface roughness characterization*, *Applied Optics,* Vol. 41, No. 10, pp. 2008-2014

Leonard, L. C. (1998). *Roughness measurement of metallic surfaces based on the laser speckle contrast method*, *Optics and Lasers in Engineering,* Vol. 30, No. 5, pp. 433-440

Leveque, J. L. (1999). *EEMCO guidance for the assessment of skin topography. The European Expert Group on Efficacy Measurement of Cosmetics and other Topical Products*, *J Eur Acad Dermatol Venereol,* Vol. 12, No. 2, pp. 103-114

Leveque, J. L. & Querleux, B. (2003). *SkinChip, a new tool for investigating the skin surface in vivo*, *Skin Res Technol,* Vol. 9, No. 4, pp. 343-347

Levy, J. L.; Servant, J. J. & Jouve, E. (2004). *Botulinum toxin A: a 9-month clinical and 3D in vivo profilometric crow's feet wrinkle formation study*, *J Cosmet Laser Ther,* Vol. 6, No. 1, pp. 16-20

Li, L.; Mac-Mary, S.; Marsaut, D.; Sainthillier, J. M.; Nouveau, S.; Gharbi, T.; de Lacharriere, O. & Humbert, P. (2006a). *Age-related changes in skin topography and microcirculation*, *Arch Dermatol Res,* Vol. 297, No. 9, pp. 412-416

Li, Z.; Li, H. & Qiu, Y. (2006b). *Fractal analysis of laser speckle for measuring roughness*, *SPIE,* Vol. 6027, pp. 60271S

Lu, R.-S.; Tian, G.-Y.; Gledhill, D. & Ward, S. (2006). *Grinding surface roughness measurement based on the co-occurrence matrix of speckle pattern texture*, *Applied Optics,* Vol. 45, No. 35, pp. 8839–8847

Lukaszewski, K.; Rozniakowski, K. & Wojtatowicz, T. W. (1993). *Laser examination of cast surface roughness*, *Optical Engineering,* Vol. 40, No. 9, pp. 1993-1997

Markhvida, I.; Tchvialeva, L.; Lee, T. K. & Zeng, H. (2007). *The influence of geometry on polychromatic speckle contrast*, *Journal of the Optical Society of America A,* Vol. 24, No. 1, pp. 93-97

Mazzarello, V.; Soggiu, D.; Masia, D. R.; Ena, P. & Rubino, C. (2006). *Melanoma versus dysplastic naevi: microtopographic skin study with noninvasive method*, *J Plast Reconstr Aesthet Surg,* Vol. 59, No. 7, pp. 700-705

Ning, Y. N.; Grattan, K. T. V.; Palmer, A. W. & Meggitt, B. T. (1992). *Coherence length modulation of a multimode laser diode in a dual Michelson interferometer configuration*, *Applied Optics,* Vol. 31, No. 9, pp. 1322–1327

Parry, G. (1984). Speckle patterns in partially coherent light. In: *Laser Speckle and Related Phenomena, Dainty, J. C.* (Eds), pp. 77-122, Springer-Verlag, Berlin; New York

Peters, J. & Schoene, A. (1998). *Nondestructive evaluation of surface roughness by speckle correlation techniques*, *SPIE,* Vol. 3399, pp. 45-56

Phillips, K.; Xu, M.; Gayen, S. & Alfano, R. (2005). *Time-resolved ring structure of circularly polarized beams backscattered from forward scattering media, Optics Express,* Vol. 13, No. 20, pp. 7954-7969

Rapini, R. (2003). Clinical and Pathologic Differential Diagnosis. In: *Dermatology, Bolognia, J. L., Jorizzo, J. L. and Rapini, R. P.* (Eds), Mosby, London

Rohr, M. & Schrader, K. (1998). *Fast Optical in vivo Topometry of Human Skin (FOITS) - Comparative Investigations with Laser Profilometry, SOFW Journal,* Vol. 124, pp. 52-59

Rosén, B.-G.; Blunt, L. & Thomas, T. R. (2005). *On in-vivo skin topography metrology and replication techniques, Phys.: Conf. Ser.,* Vol. 13, pp. 325-329

Salomatina, E.; Jiang, B.; Novak, J. & Yaroslavsky, A. N. (2006). *Optical properties of normal and cancerous human skin in the visible and near-infrared spectral range, J Biomed Opt,* Vol. 11, No. 6, pp. 064026

Sankaran, V.; Everett, M. J.; Maitland, D. J. & Walsh, J. T., Jr. (1999). *Comparison of polarized-light propagation in biological tissue and phantoms, Opt Lett,* Vol. 24, No. 15, pp. 1044-1046

Segger, D. & Schonlau, F. (2004). *Supplementation with Evelle improves skin smoothness and elasticity in a double-blind, placebo-controlled study with 62 women, J Dermatolog Treat,* Vol. 15, No. 4, pp. 222-226

Setaro, M. & Sparavigna, A. (2001). *Irregularity skin index (ISI): a tool to evaluate skin surface texture, Skin Res Technol,* Vol. 7, No. 3, pp. 159-163

Sprague, R. A. (1972). *Surface Roughness Measurement Using White Light Speckle, Applied Optics,* Vol. 11, No. 12, pp. 2811-2816

Stockford, I. M.; Morgan, S. P.; Chang, P. C. & Walker, J. G. (2002). *Analysis of the spatial distribution of polarized light backscattered from layered scattering media, J Biomed Opt,* Vol. 7, No. 3, pp. 313-320

Tchvialeva, L.; Zeng, H.; Lui, H.; McLean, D. I. & Lee, T. K. (2008). Comparing in vivo Skin surface roughness measurement using laser speckle imaging with red and blue wavelengths, *The 3rd world congress of noninvasive skin imaging*, pp. Seoul, Korea, May 7-10, 2008

Tchvialeva, L.; Zeng, H.; Markhvida, I.; Dhadwal, G.; McLean, L.; McLean, D. I. & Lui, H. (2009). Optical discrimination of surface reflection from volume backscattering in speckle contrast for skin roughness measurements, *Proc of SPIE BiOS 7161* pp. 71610I-716106, San Jose, Jan. 24-29, 2009

Contact

Tim K. Lee, PhD
BC Cancer Research Centre
Cancer Control Research Program
675 West 10th Avenue
Vancouver, BC
Canada V5Z 1L3
Tel: 604-675-8053
Fax: 604-675-8180
Email: tlee@bccrc.ca

New Developments in Biomedical Engineering

Edited by Domenico Campolo

ISBN 978-953-7619-57-2
Hard cover, 714 pages
Publisher InTech
Published online 01, January, 2010
Published in print edition January, 2010

Biomedical Engineering is a highly interdisciplinary and well established discipline spanning across engineering, medicine and biology. A single definition of Biomedical Engineering is hardly unanimously accepted but it is often easier to identify what activities are included in it. This volume collects works on recent advances in Biomedical Engineering and provides a bird-view on a very broad field, ranging from purely theoretical frameworks to clinical applications and from diagnosis to treatment.

How to reference

In order to correctly reference this scholarly work, feel free to copy and paste the following:

Lioudmila Tchvialeva, Haishan Zeng, Igor Markhvida, David I McLean, Harvey Lui and Tim K Lee (2010). Skin Roughness Assessment, New Developments in Biomedical Engineering, Domenico Campolo (Ed.), ISBN: 978-953-7619-57-2, InTech, Available from: http://www.intechopen.com/books/new-developments-in-biomedical-engineering/skin-roughness-assessment

INTECH
open science | open minds

InTech Europe
University Campus STeP Ri
Slavka Krautzeka 83/A
51000 Rijeka, Croatia
Phone: +385 (51) 770 447
Fax: +385 (51) 686 166
www.intechopen.com

InTech China
Unit 405, Office Block, Hotel Equatorial Shanghai
No.65, Yan An Road (West), Shanghai, 200040, China
中国上海市延安西路65号上海国际贵都大饭店办公楼405单元
Phone: +86-21-62489820
Fax: +86-21-62489821